PHYSICAL REVIEW B VOLUME 27, NUMBER 8 15 APRIL 1983

Electrical transport in low-resistivity amorphous metals

L. V. Meisel and P. J. Cote
U.S. Army Armament Research and Development Command, Large Caliber Weapon Systems Laboratory, Benet Weapons Laboratory, Watervliet, New York 12189
(Received 3 November 1982; revised manuscript received 12 January 1983)

Diffraction-model calculations incorporating appropriate scattering matrix elements and phonon-ineffectiveness effects (saturation effects) yield results which are consistent with the observed temperature dependence of the electrical resistivity in low-resistivity ($\rho < 100\ \mu\Omega$ cm) amorphous alloys. In particular, remarkably good quantitative agreement with available detailed resistivity measurements in *a*-MgZn alloys has been obtained by these methods. The results further indicate that saturation effects, which dominate the temperature dependence of the high-resistivity amorphous metals, are important even for resistivities as low as 50 $\mu\Omega$ cm.

I. INTRODUCTION

Most quantitative theoretical results on electrical transport in amorphous metals have been obtained using the diffraction model[1–6] and its extensions[6–11] in which the electron-phonon interaction matrix element is assumed to be independent of the electron mean free path. We shall refer to such calculations in this paper as applications of the *standard* diffraction model. The standard diffraction model also serves as the basis for the analysis of transport in crystalline metals, yielding Bloch-Gruneisen theory[12] for normal scattering processes. However, the standard diffraction model is of questionable validity for most amorphous metals whose resistivities are of the order of or greater than 150 $\mu\Omega$ cm, which corresponds to electron mean free paths of the order of ionic spacings. The deviations of experimental results from the predictions of the standard diffraction model in high-resistivity metals are referred to as "saturation effects" or Mooij phenomena.[6,13–17] In spite of the presence of saturation effects, the standard diffraction model gives reasonable values for the magnitude of the electrical resistivity and its concentration dependence in a number of amorphous alloys[6,18]; in fact, the model is often not observed to fail unless close attention is paid to details of the temperature dependence of the resistivity. We refer to treatments of electrical transport in which the electron-phonon interaction is electron mean-free-path dependent[16,17] as "saturated cases" of the diffraction model.

The treatment of Mooij phenomena has been the subject of considerable theoretical study. Some investigators have treated high-resistivity metals in the context of the diffraction model by postulating interband tunneling channels[19] or, in analogy with the Pippard theory of ultrasonic attenuation in metals,[20] an electron mean-free-path—dependent electron-phonon interaction.[16,17] Other investigators[21] have approached the problem by extending theories intended for transport in materials whose electrons are localized.

The standard diffraction model is expected to be valid when the electron mean free path is not too short. Thus, a test of the theory in low-resistivity ($\rho < 100\ \mu\Omega$ cm) metallic glasses is of interest. Until recently relatively few experiments have been performed on such alloys since they are difficult to fabricate. Notable exceptions were the results in vapor-deposited *a*-CuSn (Ref. 22) and *a*-AuSn (Ref. 23) alloys for a wide range of compositions. These alloys exhibit the features predicted by the diffraction model including trends in ρ and the temperature coefficient of resistivity (TCR) with composition, and the presence of a maximum in ρ vs T in alloys with a negative room-temperature TCR, an essential feature of standard-diffraction-model predictions.[6]

There are now substantial data for low-resistivity amorphous alloys. Matsuda and Mizutani completed a thorough study of electrical transport in *a*-MgZn alloys[24] from 2—300 K with Zn concentrations ranging from 22.5 to 35 at.% and in an *a*-MgCu alloy.[25] Mizutani and Yoshida[26] provided data on a variety of Ag-Cu—based alloys from 77—300 K. Earlier, Hafner *et al.*[27] had found good agreement between experiment and the theory of Refs. 7—9 in a preliminary study on *a*-Mg_7Zn_3. These alloys are particulary suited for tests of the diffraction model because of their low resistivities ($\sim 50\ \mu\Omega$ cm) and the existence of supporting data which determine the relevant parameters in the Ziman-Faber theory (e.g., Fermi wave number k_F

and structure-factor peak position k_p). Moreover, the conduction-electron states in a-MgZn may be assumed to be almost exclusively of s and p character in contrast to the complex situation in the more common transition-metal–based glassy alloys.

In this paper we compare the a-MgZn–alloy transport data with results computed using the diffraction model with (i) Heine-Aberenkov pseudopotentials as tabulated by Harrison[28] used for the scattering matrix element in the Born approximation, and (ii) a phase-shift expansion of the scattering matrix elements as developed by Evans *et al.*[29] Saturation effects are taken into account by invoking the Pippard-Ziman constraint on the electron-phonon interaction.[1,6,16,17] A brief review of the theory is given in Sec. II. The scattering potential is discussed in Sec. III where the method of selecting phase shifts appropriate for a-MgZn is described and problems encountered with the Born approximation are discussed. In Sec. IV a detailed comparison is made between the data on a-MgZn and the predicted results using the diffraction model with both the phase-shift expansion and pseudopotential scattering matrix elements. Implications for transport in general low-resistivity alloys are also described in Sec. IV. A summary and conclusions are given in Sec. V.

II. THEORY

The diffraction model (Ziman-Faber theory[5]) result for the electrical resistivity is

$$\rho=\frac{12\pi\Omega_0}{e^2\hbar V_F^2}\int_0^1 d\left[\frac{K}{2k_F}\right]\left[\frac{K}{2k_F}\right]^3 S^\rho(K)\,|\,u(K)\,|^2\,, \tag{1}$$

where Ω_0 is the atomic volume, V_F is the Fermi velocity, k_F is the Fermi wave vector, K is the scattering vector, $\hbar$ is Planck's constant divided by 2π, e is the electron charge, and the resistivity static structure factor $S^\rho(K)$ is defined in terms of the Van Hove dynamical structure factor[4] $S(K,\omega)$ as

$$S^\rho(K)=\int_{-\infty}^{\infty} d\omega\, xn(x)S(K,\omega)\,, \tag{2}$$

where $x=\hbar\omega/k_BT$, $n(x)=(e^x-1)^{-1}$, k_B is Boltzmann's constant, and T is the absolute temperature. The scattering matrix element $u(K)$ is approximated by a pseudopotential in the Born approximation, or for strong scattering (i.e., large phase shifts) it can be expressed in terms of phase shifts[29] as

$$u(K)=\frac{2\pi\hbar^3}{m(2mE_F)^{1/2}\Omega_0}\sum_l (2l+1)\sin[\eta_l(E_F)]e^{i\eta_l(E_F)}P_l(\cos\theta)\,, \tag{3}$$

where the phase shift $\eta_l(E_F)$ for angular momentum quantum number l is evaluated at the Fermi energy and m is the electron mass. The matrix element in the form of Eq. (3) includes single-site multiple scattering and is called the t matrix. We shall discuss transport in a-MgZn alloys using both of these formulations. The general case is described in terms of the t matrix.

The resistivity static structure factor in an amorphous Debye solid may be expanded in the form[6–9]

$$S^\rho(K)=S_0^\rho(K)+S_1^\rho(K)+S_2^\rho(K)+\cdots\,, \tag{4}$$

where $S_n^\rho(K)$ is an n-phonon term. The elastic scattering term (no phonons) is

$$S_0^\rho(K)=a(K)e^{-2W(K)}\,, \tag{5}$$

where $e^{-2W(K)}$ is the Debye-Waller factor and the geometrical structure factor $a(K)$ is

$$a(K)=\frac{1}{N}\sum_{m,n}\exp[i\bar{K}\cdot(\bar{m}-\bar{n})]\,, \tag{6}$$

with m,n being averaged ionic positions. The one-phonon term allowing for Pippard-Ziman phonon ineffectiveness as described in Refs. 16 and 17 is

$$S_1^\rho(K)=\alpha(K)e^{-2W(K)}\frac{T}{\Theta}\int_0^1 d\left[\frac{q}{q_D}\right]\left[\frac{q}{q_D}\right]^2 n(x)[n(x)+1]\int\frac{d\Omega_q}{4\pi}a(\,|\bar{K}+\bar{q}\,|\,)F(q\Lambda)\,, \tag{7}$$

where $\alpha(K)=3(\hbar K)^2/Mk_B\Theta$ where M is the averaged ionic mass, q_D is the Debye wave number, Θ is the Debye temperature, $x=(\Theta/T)(q/q_D)$ for a Debye solid, Λ is the electron mean free path, and $F(q\Lambda)$ describes the reduction in scattering effectiveness which occurs for small $q\Lambda$. The calculations presented here assume that $F(q\Lambda)$ can be represented by the form suggested by Pippard[20] in

his study of ultrasonic attenuation, and

$$F(y)\equiv\frac{2}{\pi}\left[\frac{y\tan^{-1}y}{y-\tan^{-1}y}-\frac{3}{y}\right]\text{ (Pippard saturation) .} \tag{7a}$$

We refer to this expression as the Pippard function. If saturation effects can be ignored,

$$F(y)=1\text{ (no saturation) .} \tag{7b}$$

We refer to this form of the theory as the standard diffraction model. Equation (7b) is also clearly the long electron mean-free-path limit (or low-resistivity limit) of the Pippard function. One can also represent saturation effects with a "sharp cutoff" form

$$F(y)=\begin{cases}0, & y<y_c\\ 1, & y>y_c\end{cases}\text{ (sharp cutoff) ,} \tag{7c}$$

where the cutoff value y_c is of order $q_D a$ where a is the mean ionic spacing. Note that the placement of $F(q\Lambda)$ in the one-phonon part of the (generalized) resistivity static structure factor results from a decomposition of the absolute square of a phonon wave number and electron mean-free-path–dependent electron-phonon matrix element into a simple product according to the prescription

$$|u(K,q\Lambda)|^2=|u(K)|^2F(q\Lambda) ,$$

where $u(K)$ is the ordinary scattering matrix element which appears, for example, in the elastic scattering term.

The multiphonon series is approximated in various ways.[30] For the range of temperatures of interest here ($T\lesssim\Theta$) the particular approximation made is not important and the results are given in Sham-Ziman approximation,[30] i.e., we assume that the effect of the multiphonon series is to cancel the Debye-Waller factor in the one-phonon term. We shall refer to that modified term as the inelastic scattering term or simply the phonon scattering term.

The Debye-Waller exponent is given (for a Debye solid) by

$$2W(K)=\alpha(K)\int_0^1 d\left[\frac{q}{q_D}\right]\left[\frac{q}{q_D}\right][n(x)+\tfrac{1}{2}] \tag{8a}$$

$$=\alpha(K)\left[\frac{T}{\Theta}\right]^2\int_0^{\Theta/T}dx\,x[n(x)+\tfrac{1}{2}] . \tag{8b}$$

Note that Eqs. (1)–(8) have been written in a form appropriate to a pure substance. The product $S^{\rho}(K)|u(K)|^2$ should be replaced by a sum of concentration-dependent terms involving individual constituent scattering matrix elements and partial structure factors in alloy systems. Nevertheless, in the a-MgZn alloys we treat the material with a single effective scattering potential in the spirit of the substitutional model of Faber and Ziman[5] and a Percus-Yevick form[31] for the geometrical structure factor. This is not quite right when there is short-range order and $2k_F$ is situated differently with respect to the peak positions of the various partial structure factors. However, a broad range of scattering vectors contribute to the resistivity in a-MgZn, the constitutents have very similar atomic structure, and the computations by von Heimendal[32] suggest that the three partial structure factors are very similar; we thus assume that the conditions for the substitutional model apply. The application of the substitutional model to the other low-resistivity amorphous alloys considered here may not be as good an approximation.

III. THE SCATTERING MATRIX ELEMENT AND THE MAGNITUDE OF ρ

The atomic structure of Mg consists of filled shells and $3s^2$ electrons, and similarly in Zn, filled shells and $4s^2$ electrons. It follows from straightforward considerations of the atomic structure of these simple divalent metals that the appropriate starting structure in the metallic solid will consist of a nearly filled s band with some p-band occupation resulting in a metallic sp band primarily of s character with a small admixture of p character. (Note that the energy required to promote an electron to a d level in Mg or Zn is prohibitively large in contrast to the situation in Ca, Sr, or Ba.) Thus if we construct a scattering matrix element as given in Eq. (3), we expect the s-wave phase shift $\eta_0(E_F)$ to be slightly less than π, the p phase shift $\eta_1(E_F)$ to be small, and other phase shifts to be negligible. Such a scattering matrix element will be drastically different in form from a Born-approximation pseudopotential matrix element. We have constructed such a matrix element for a-MgZn by adjusting $\eta_0(E_F)$ to give the observed magnitude of ρ with $\eta_1(E_F)$ constrained to satisfy the Friedel sum rule.[33] (Since there are only $l=0$ and 1 phase shifts to consider and the electron per atom ratio, $z=2$, one has to satisfy $\eta_0+3\eta_1=\pi$.) The resulting values of $\eta_0(E_F)$ and $\eta_1(E_F)$ are 2.87 and 0.09, respectively; we use these values in our subsequent investigations of the temperature dependences.

Dunsworth[34] has deduced phase shifts for Zn in β brasses by adjusting augmented-plane-wave– (APW) form matrix elements to fit experimentally determined Fermi-surface features. His results for Zn in crystalline β brasses where $z=1.5$ electrons per

atom are $\eta_0=3.114$, $\eta_1=0.289$, and $\eta_2=0.001$ at the free-electron Fermi energy. This lends support to our general expectation that the divalent metals and alloys will exhibit large $l=0$ phase shifts (near π) and small $l=1$ phase shifts.

It should be stressed that although the magnitude of ρ is quite sensitive to changes in the phase shifts, the T dependence of $\rho(T)/\rho(\Theta)$ is relatively insensitive to specific phase-shift values. For example, a matrix element constructed for $\eta_0=2.00$ and $\eta_1=0.38$ yields a factor-of-2 increase in ρ but only changes the temperature dependence of $\rho(T)/\rho(\Theta)$ by about 5% over the range from 0 K to Θ for the values of $2k_F/k_p$ studied here. In fact, for $\pi/2\lesssim\eta_0\lesssim\pi$ and η_1 adjusted to satisfy the sum rule, the scattering matrix elements are similar in form to that shown in Fig. 1 for $\eta_1=2.87$ and give essentially equivalent (i.e., within about 20%) temperature dependences for $\rho(T)/\rho(\Theta)$.

Another point which should be considered is the effect on $\rho(T)$ of breakdown of the Freidel–sum-rule constraint. Although various forms of the Friedel sum rule[35,36] are invoked to constrain phase shifts evaluated at the Fermi energy, it should be noted that calculated phase shifts often fail to satisfy the sum rule; for example, in Ref. 36 the phase shifts computed for Ca and Sr yield Freidel sums differeing by 15% and 3%, respectively, from the sum rule. Again the form of the t matrix [which determines the temperature dependence of $\rho(T)/\rho(\Theta)$] is preserved even for potentials which do not satisfy the sum rule as long as $\pi/2\lesssim\eta_0\lesssim\pi$ and η_1 is not too large.

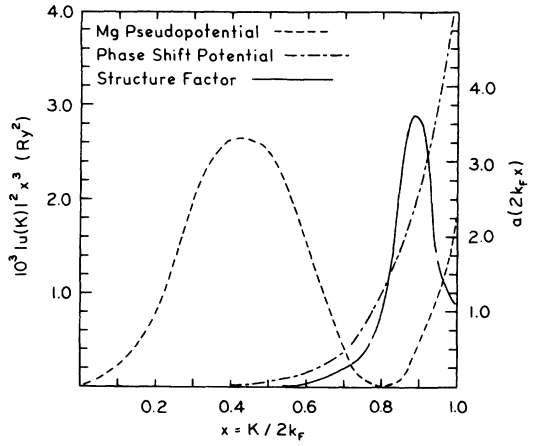

FIG. 1. Weighted absolute squared scattering matrix elements used to describe transport in a-MgZn. Mg pseudopotential is from Ref. 28. Phase-shift-expanded matrix element is adjusted as described in the text for use in a-MgZn. Percus-Yevick hard-sphere structure factor with parameters appropriate to approximate the geometrical structure factor $a(K)$ in a-MgZn is also shown for the case where $2k_F=1.1k_p$. Note that the inelastic part of the resistivity static structure factor $S^\rho(K)$ will be substantially broader than $a(K)$ for $T\approx\Theta$ and that the δ function in $a(K)$ at $K=0$ is not represented.

The point of this discussion is that although the phase shifts deduced for a-MgZn are not uniquely determined by the transport data, the temperature dependence of the resistivity of all the low-resistivity amorphous alloys studied to date can be discussed in terms of an approximate t matrix of the form shown in Fig. 1. Also one might expect the best phase shifts for a-MgZn to be given within about the deviations from the sum rule seen in Ca or Sr.

If one uses the Born approximation with Heine-Aberenkov pseudopotentials as tabulated in Ref. 28 for Mg and Zn, approximates $S^\rho(K)$ by $S_0(K)$, and takes a value of k_F appropriate to the a-MgZn alloys, then one obtains 20 and 29 $\mu\Omega$ cm, respectively, for the Mg and Zn pseudopotentials. The discrepancy between either of these values and the measured resistivities of the a-MgZn alloys is of the order found when those methods have been applied to transport in liquid metals.[37] However, the form of the Born-approximation matrix element is drastically different from that of the adjusted phase-shift matrix element as may be seen in Fig. 1. The cancellation near $2k_F$, which is characteristic of pseudopotentials, does not occur in the phase-shift-expanded matrix element.

Considering only the theoretical results for the magnitude of ρ, either approach can yield reasonable agreement with the data in a-MgZn alloys. However, we shall see in Sec. IV that the phase-shift matrix element leads to a better approximation to the observed temperature dependence in a-MgZn than the Born-approximation results.

Moreover, there are well-known examples of difficulties with Born-approximation transport calculations in related systems. For example, the electrical resistivity computed with Heine-Aberenkov pseudopotentials in the Born approximation and with Percus-Yevick hard-sphere structure factors is in poor agreement with experiment in liquid Ca, Ba, and Sr. On the other hand, Ratti and Evans[38] obtained good agreement with the experimental data in liquid Ca, Ba, and Sr using a phase-shift-expanded form for the scattering matrix element [Eq. (3)] with phase shifts computed from muffin-tin potentials. (The only significant phase shifts in these alkaline-earth liquids were an s phase shift slightly less than π and a small d phase shift.)

Furthermore, there are even indications of difficulties with the Born approximation for the treatment of transport in monovalent liquid metals. Young *et al.*[36] concluded that Born approximation

was inadequate in these liquid metals and achieved improved agreement with electrical resisitivity and thermopower in terms of phase-shift-expanded matrix elements [Eq. (3)]. In the light of these findings for liquid Ca, Ba, and Sr, and for the liquid monovalent metals, it is perhaps not surprising that we find that the temperature dependence of the electrical resistivity in a-MgZn and the other low-resistivity amorphous alloys is better described by a scattering matrix element of the form of Eq. (3) (t matrix) than by pseudopotentials in the Born approximation.

IV. COMPARISON OF THEORETICAL AND EXPERIMENTAL RESULTS

The parameters used in the computations are listed in Table I. They are based upon the following: x-ray and neutron diffraction[39] yield values of k_p in a-Mg_7Zn_3 of 2.7 and 2.6 Å^{-1}, respectively. Hall-effect measurements by Matsuda and Mizutani[24] give $2.77 < 2k_F < 2.98$ Å^{-1} for the range of compositions of a-MgZn studied. The mean ionic mass is used for M and in a-MgZn we take $q_D = k_F$ (since $z=2$). Specific-heat measurements[40] in a-Mg_7Zn_3 yield $\Theta = 295$ K. We have also assumed a Debye phonon spectrum and an effective (geometric) structure factor of Percus-Yevick form with packing fraction $\eta = 0.525$ (which is representative of structure factors found in amorphous alloys).

In the remainder of this paper, when we refer to the *saturated case,* we are quoting results computed for Pippard saturation with $q_D\Lambda = 11.7$ in Eq. (7a) which produces a 25% reduction in the inelastic scattering part of the resistivity at $T=\Theta$. (This is equivalent to assuming the saturation resistivity $\rho^* \approx 200$ $\mu\Omega$ cm in the treatment of Ref. 17.) We emphasize here that inelastic scattering contributes less than 5% to the total ρ so that the effect of saturation in the adjusted phase shifts is negligible. The unsaturated case results are obtained from the standard diffraction model, i.e., using Eq. (7b) or letting $\Lambda \to \infty$ in Eq. (7a).

Table II summarizes many of the principal experimental results regarding electrical transport for $T \lesssim \Theta$ in a-MgZn and also in a-AuSn and a-CuSn alloys along with corresponding theoretical results based upon Mg and Zn pseudopotentials and the adjusted phase-shift matrix elements for the saturated and unsaturated cases. Generally, the adjusted phase-shift matrix element in the unsaturated case yields better agreement with the detailed experimental results than the Born-approximation results and the phase-shift results including saturation yield the best agreement with experiment in the a-MgZn alloys. Furthermore, there is excellent qualitative agreement between the phase-shift results and the amorphous noble-metal–based data. These results strongly suggest that saturation effects or Mooij phenomena are readily observable in amorphous alloys with resistivity as low as $50\,\mu\Omega$ cm.

Let us now turn to a brief description of our results for the various temperature regions studied in detail by Matsuda and Mizutani[24] in a-MgZn and the overall temperature dependences predicted for the other known low-resistivity amorphous alloys.

A. Room-temperature ($T \approx \Theta$) TCR

The high-temperature ($T \gtrsim \Theta$) form for the (effective) resistivity static structure factor to first order in $\alpha(K)$ is

$$S^{\rho}(K) \cong a(K)e^{-\alpha(K)/4} + \alpha(K)(T/\Theta) \times [A^{\rho}(K)(1-\gamma) - a(K)e^{-\alpha(K)/4}] , \quad (9)$$

where $\gamma = 0$ in the standard diffraction model (i.e., no saturation) and for Pippard or sharp-cutoff saturation, $\gamma \approx \rho/\rho^*$. Generally, $\rho^* \approx 200$ $\mu\Omega$ cm in high-resistivity systems[14–17] and so we have taken $\gamma \approx \frac{1}{4}$ in a-MgZn. This was the basis for our choice

TABLE I. Summary of input for resistivity calculations in a-MgZn. The Debye temperature Θ was determined from specific-heat measurements (Ref. 40), the position of the first peak in the structure factor k_p was determined by neutron diffraction (Ref. 39) and the Fermi wave numbers k_F were deduced from Hall-effect measurements (Ref. 24). η is the hard-sphere packing fraction in the Percus-Yevick formula (Ref. 37).

Input	Description	Parameters
Phonon spectrum	Debye form	$\Theta = 295$ K $q_D = k_F$
Geometrical structure factor	Percus-Yevick Hard-sphere form	$\eta = 0.525$ $k_p = 2.6$ Å^{-1}
Fermi wave numbers	For Zn concentration: 0.225, $2k_F = 2.77$ Å^{-1} For Zn concentration: 0.35, $2k_F = 2.98$ Å^{-1}	

TABLE II. Summary of theoretical and experimental results in low-resistivity amorphous alloys. The "Brillouin scattering part" refers to the part of the TCR arising from the δ function at $K=0$ in $a(K)$. The values of $2k_F$ and k_p and hence $2k_F/k_p$ in the a-MgZn alloys were experimentally determined; the values of $2k_F/k_p$ given for a-CuSn are nearly free-electron (NFE) values and are consistent with the concentration dependence of ρ; the concentration dependence of ρ in a-AuSn suggests that $2k_F/k_p$ is $\sim 10\%$ less than NFE values. Coefficient A is defined by $\rho \approx \rho_0(1+AT^2)$ for $5<T<40$ K. Coefficient B is defined by $\rho \approx \rho_1 - BT^{3/2}$ for $T_M < T < 240$ K. Column headed Avg. lists average values for the alloys studied in Ref. 24.

Alloy	a-MgZn Theory				a-MgZn Expt.			a-CuSn Expt.		a-AuSn Expt.	
z	2				2			1.6	3.4	1.6	3.4
$2k_F/k_p$	1.11				Avg.	1.06	1.15	~ 1.0	~ 1.3		
Potential	Pseudo		Phase shift								
	Mg	Zn									
$q_D\Lambda$	∞	∞	∞	11.7							
$\rho(\Theta)$ ($\mu\Omega$ cm)	20	29	53	53	53	49	57	112	65	99	60
10^4 TCR(Θ)(K^{-1})	−0.05	1.0	−0.97	−1.2	−1.9	−1.5	−2.0	−1.3	0.6	−1.4	0.8
10^4 (Brillouin part)	0.32	0.40	2.7×10^{-4}								
T_M (K)	>150	None	90	46	47	55	40	Monotonic		18	43
$10^3[\rho(T_M)/\rho(0\text{ K})-1]$			3.0	0.62	0.69	1.11	0.37	at extremes			
10^4B ($\mu\Omega$ cm $K^{-3/2}$)				3.7	4.5	3.5	5.5				
10^6A (K^{-2})			1.01	0.48	0.50						

of $q_D\Lambda=11.7$ in Pippard saturation. The high-temperature limiting form of the averaged resistivity structure factor $A^\rho(K)$ as defined in Refs. 6–9 is given by

$$A^\rho(K)=\int_0^1 d\left[\frac{q}{q_D}\right]\int\frac{d\Omega q}{4\pi}a(|\bar{K}+\bar{q}|)\,. \quad (10)$$

The sign of the contribution to the TCR from scattering vector K is determined by

$$A^\rho(K)(1-\gamma)-a(K)e^{-\alpha(K)/4}\,.$$

In the extreme backscattering case (as is often assumed for transition-metal–based amorphous alloys) one has $\rho \propto S^\rho(2k_F)$ and the TCR is negative if

$$a(2k_F)e^{-\alpha(2kF)/4} > A^\rho(2k_F)(1-\gamma)\,.$$

In particular, for no saturation and Percus-Yevick structure factors with packing fraction 0.525 (appropriate for a large class of amorphous metals), negative TCR would be predicted for $0.9 \lesssim 2k_F/k_F \lesssim 1.1$. On the other hand, when a relatively broad range of scattering vectors yield significant contributions to ρ and the TCR, one must employ Eq. (1) to determine $\rho(T)$, and this simple criterion for the occurrence of negative TCR is invalid. Saturation effects will also invalidate this criterion; the range of $2k_F/k_p$ for negative TCR is increased when $\gamma>0$ and negative TCR will generally occur for all $2k_F/k_p$ values when $\gamma \gtrsim 0.5$.

The computed TCR's in a-MgZn are listed in Table II for the various conditions considered. The "Brillouin scattering" contribution,[6,10] which arises from the δ function at $K=0$ in $a(K)$ and gives the normal scattering contribution in the crystalline case, is listed separately in Table II to indicate the relative importance of this term. (We have generally assumed that Brillouin scattering contributions are negligible in transition-metal–based amorphous alloys since backscattering is expected to dominate.) The following interesting features are indicated.

(i) The range of $2k_F/k_p$ for which negative TCR's are predicted with the phase-shift approximation in Eq. (1) is shifted toward considerably higher values than those given in the extreme backscattering case. The Mg pseudopotential results suggest a similar but smaller shift. The range of $2k_F/k_p$ for a negative TCR in saturated and unsaturated cases (excluding the Zn pseudopotential case) are consistent with the data of Ref. 24. Negative TCR values were obtained for $0.96 \lesssim 2k_F/k_p \lesssim 1.24$ in the unsaturated case; the range when saturation effects ($q_D\Lambda=11.7$) are included is $0.94 \lesssim 2k_F/k_p \lesssim 1.29$.

(ii) The computed Brillouin scattering contribution to the TCR is negligible in the phase-shift formulation, but is significant in the Born-approximation case. For the Zn pseudopotential, negative TCR's are essentially eliminated by the Brillouin contribution for all k_F. Froböse and Jäckle[10] had encountered similar difficulties with their Born-approximation calculations on a-CuSn.

(iii) The Born-approximation results for the TCR are in poor agreement with experiment. The phase-shift results are about half as large as the observed TCR.

B. Low-temperature T^2 region, minima, and maxima in $\rho(T)$

The low-temperature limiting form of the resistivity static structure factor[6–9] neglecting saturation is

$$S^{\rho}(K)=a(K)+(\pi^2/6)a(K)\alpha(K)(T/\Theta)^2 . \quad (11)$$

Thus the standard diffraction model yields a positive quadratic temperature dependence for the resistivity near 0 K, independent of the sign of the TCR at high temperatures. Consequently, a general feature of the standard diffraction model is that if the room-temperature TCR is negative, the resistivity will exhibit small maxima in $\rho(T)$. (This simple result is often ignored, leading to improper conclusions regarding agreement between theory and experiment in high-resistivity amorphous alloys.) Matsuda and Mizutani[24] observed a quadratic $\rho(T)$ in a-MgZn below 30 K which they attribute to the low-temperature form of the theory based upon Eqs. (1) and (11). However, detailed calculations indicate that significant deviations from Eq. (11) occur above about 5 K for K near k_p so this interpretation is questionable; in particular, the low-temperature limit of the T^2 coefficient will generally not be observed above ~ 5 K. Nevertheless, the standard diffraction-model results for a-MgZn are consistent with a quadratic $\rho(T)$ in the range 5–30 K. However, the computed coefficient of the quadratic term, given in Table II, is smaller than the low-temperature limit (which is about 2×10^{-6} K^{-2}) in the unsaturated case but is still larger than the measured coefficient by a factor of 2. When saturation is included, excellent agreement with the measured coefficient is obtained.

Figure 2 shows the ρ-vs-T curves obtained by Matsuda and Mizutani[24] for a-MgZn alloys between 2 and 70 K. Small maxima in the resistivity $[\rho(T_M)-\rho(0\text{ K})\approx 10^{-3}\rho(0\text{ K})]$ are observed for $T_M\approx 50$ K where T_M is the temperature at the resistivity maxima. Figure 3(a) shows phase-shift–based standard diffraction-model results. The $2k_F/k_p=1.1$ case is appropriate for a-MgZn and is in qualitative agreement with the experimental results shown in Fig. 2. However, the computed maximum occurs at $T_M\approx 0.3\Theta$, which corresponds to $T_M\approx 90$ K, and the computed maximum is substantially larger than observed. When saturation is included, excellent agreement [see Table II and Fig. 3(b)] in the position and size of the maximum is obtained. The Born-approximation results at these temperatures are in very poor agreement with experiment.

The data of Fig. 2 exhibit another interesting feature, viz., small minima at about 10 K. This feature is *not* consistent with standard diffraction-model predictions. However, as may be seen in Fig. 3(b) or from the results listed in Table II, the theory including saturation is again in excellent agreement with the data. This is a particularly interesting result since to observe such effects, $q_D\Lambda$ has to be large enough to produce an observable minimum but not so large as to produce monotonic decreasing $\rho(T)$; also the alloys under investigation must be free of effects associated with magnetic ions or transitions to superconductivity. (Essentially the same results, although with deeper minima, are obtained in the case of sharp-cutoff saturation corresponding to $\gamma=\frac{1}{4}$.) It is possible, of course, that this agreement is fortuitous.

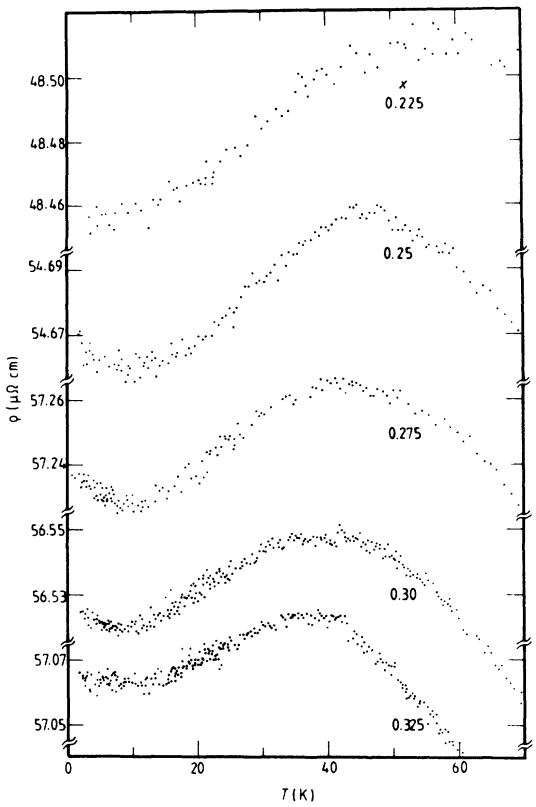

FIG. 2. Electrical resistivity vs temperature below 70 K in a-MgZn from Ref. 24.

C. Other low-resistivity amorphous alloys

Other low-resistivity ($\rho<100\,\mu\Omega$ cm) amorphous alloys with $2k_F/k_p\gtrsim 1$ that we are aware of and for which the temperature dependence of the electrical resistivity has been determined, are a-CuSn,[22] a-AuSn,[23] a-AuIn,[23] a-MgCu,[25] a-AgCuAl,[26] a-AgCuMg,[26] and a-AgCuGe.[26] These alloys have been studied over wide ranges of temperature and

composition which correspond to extensive ranges in $2k_F/k_p$; for example, for a-CuSn and a-AuSn, this range varies from about 1.0 to about 1.3. Figure 3 shows theoretical results for similar ranges in $2k_F/k_p$ in the saturated and unsaturated cases and parameters appropriate to the a-MgZn alloys.

Before the results exhibited in Fig. 3 are compared with measurements in the other alloys we make the following comments: (i) The magnitude of the variations in the electrical resistivity with T in the range from 0 K to Θ is governed essentially by $M\Theta$. Hence, although the effective masses are larger, the expected lower Debye temperatures for these noble-metal–based alloys relative to a-MgZn, can account for the fact that the temperature-dependent effects in the resistivity are of the same magnitude. (ii) The range of resistivities in the other alloys is considerably larger than in the a-MgZn alloys. Thus, we cannot expect $q_D\Lambda=11.7$ to be appropriate for all these alloys. This effect can be significant; e.g., for $\rho\approx 100\ \mu\Omega$ cm, saturation effects could completely eliminate the small maximum in $\rho(T)$, for $2k_F\approx k_p$, yielding a monotonic decreasing function. (In fact, this was observed in Ref. 23 for the a-AuSn alloy with $\rho\approx 100\ \mu\Omega$ cm.) (iii) There could be appreciable short-range-order effects produced by the differences in effective potential and application of the "substitutional model" might not be appropriate for such different ionic constituents as occur in these alloys.

In spite of these difficulties, all the low-resistivity alloy systems exhibit the general features shown in Fig. 3 including resistivity maxima in negative TCR cases. This strongly suggests that matrix elements of the form given in the phase-shift expansion rather than Born approximation pseudopotential is appropriate in these alloys. The temperature dependences of the various composition (i.e., various $2k_F/k_p$) a-CuSn alloys are in remarkable agreement with the saturated case curves in Fig. 3(b) if we use free-electron theory to compute $2k_F/k_p$ for each composition. Similar consistency is obtained for the a-AuSn data if we deduce $2k_F/k_p$ from the ρ and TCR vs composition data shown in Ref. 23 (which leads to $2k_F$ values about 10% smaller than free-electron values). The a-MgCu[25] data are essentially identical to those of a-MgZn. The AgCu-based alloys[26] offer a particularly clear illustration of the shift to higher values for the $2k_F/k_p$ range of negative TCR values.

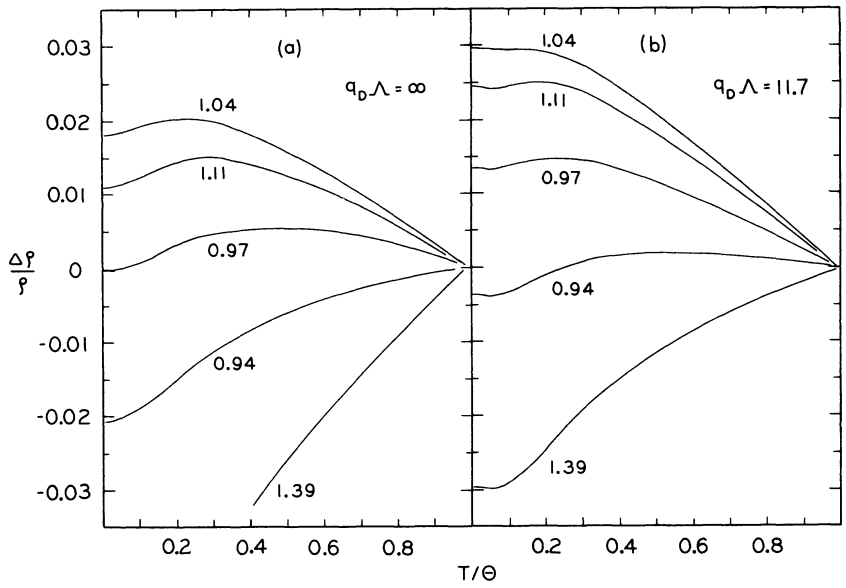

FIG. 3. Relative change in the resistivity vs T/Θ computed from the diffraction model with the adjusted phase-shift-expanded matrix element appropriate to a-MgZn. Parameter associated with each curve is $2k_F/k_p$. (a) is computed from the standard diffraction model ($\Lambda\rightarrow\infty$) and (b) includes Pippard saturation with $q_D\Lambda=11.7$. Computed resistivity values are 29, 40, 59, 53, and 22 $\mu\Omega$ cm for $2k_F/k_p=0.94$, 0.97, 1.04, 1.10, and 1.39, respectively. The range of $2k_F/k_p$ determined for the a-MgZn (Ref. 24) extends from about 1.06 to 1.15 while in a-CuSn (Ref. 22) it extends from about 1.0 to 1.3. Note particularly the larger negative TCR values, the movement of the maxima toward lower temperatures, and the appearance of minima at temperatures below 0.1Θ in the calculations including saturation. Curves in (a) should be compared with the plots of $S^{\rho}(T)/S^{\rho}(\Theta)$ vs T/Θ for various K values which are equivalent to $\Delta\rho/\rho$ vs T/Θ for various values of $2k_F$ in the "backscattering dominant" approximation in Ref. 9.

D. $(T-T_M)^{3/2}$ temperature dependence

Matsuda and Mizutani[24,25] discovered that over an extensive range of temperature to the right of T_M, the resistivity in the aMgZn and aMgCu alloys has the form

$$\rho(T)=\rho_1-B(T-T_M)^{3/2} . \quad (12)$$

The phase-shift calculation, including saturation, fits this equation, and thus the experimental data, surprisingly well both with regard to the value of B (Table II) and the linearity of the ρ-vs-$(T-T_M)^{3/2}$ plot as seen in Fig. 4.

V. SUMMARY AND CONCLUSIONS

Electrical resistivity of low-resistivity ($\rho<100$ $\mu\Omega$ cm) amorphous metals has been studied in the context of the Ziman-Faber diffraction model which has been generalized to account for saturation effects by incorporation of the "Pippard function"[20] which described the reduction of the electron-phonon interaction at small $q\Lambda$ where q is the phonon wave number and Λ is the electron mean free path. The standard diffraction-model formulas are obtained in the limit that Λ goes to infinity. (Essentially equivalent results were obtained with the use of a "sharp-cutoff" form to describe saturation effects.)

The specific computational results were obtained for a-MgZn alloys which comprise an ideal system to test the diffraction model because of their relatively simple electronic structure, low resistivity, and the existence of detailed experimental data covering temperatures from 2 to 300 K in a series of well-characterized alloys. Moreover, the similarity of the atomic structures and ionic radii of Mg and Zn allow us to make the further computational simplification of adopting the Faber-Ziman substitutional model.[5] The parameters used in the computations and listed in Table I are thus appropriate to the a-MgZn alloys.

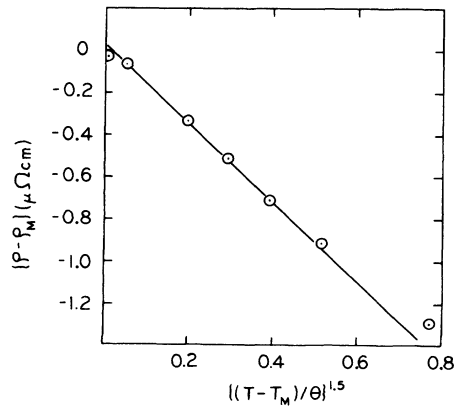

FIG. 4. $\frac{3}{2}$ power region to the right of the resistivity maximum in a-MgZn. Points are theoretical values. Line is a plot of Eq. (12). Deviations from linearity, extent of the linear region, and slope agree with the data in Ref. 24.

Pseudopotential matrix elements in the Born approximation and an adjusted phase-shift scattering matrix element were employed. The phase-shift-expanded form was assumed to include only s and p components (from consideration of the atomic structure of Mg and Zn) and the phase shifts were adjusted to yield the observed magnitude of ρ and to satisfy the Friedel sum rule. The Mg and Zn pseudopotentials were taken from Harrison.[28] These two types of matrix elements are quite different in form. The cancellation near $2k_F$, characteristic of pseudopotentials, does not appear in the adjusted phase-shift-expanded matrix element.

The adjusted phase-shift results, neglecting saturation ($\Lambda\rightarrow\infty$), are in qualitative agreement with the data, exhibiting all the observed features of the experimental data in a-MgZn except for the small minimum at about 5 K. The phase-shift results, including saturation with $q_D\Lambda=11.7$ (chosen in accordance with the ideas presented in Ref. 17), are in remarkable agreement with the observed details of the temperature dependence of the electrical resistivity in the a-MgZn alloys,[24] including the room-temperature TCR, the shape and extent of the $(T-T_M)^{3/2}$ region to the right of the maximum, the magnitude and position of the maximum, the shape and extent of the quadratic in the T region, and even the position and size of the minimum near 5 K.

We also note that negative TCR's occur at significantly higher $2k_F/k_p$ values than predicted with the extreme backscattering approximation and are consistent with the data of Refs. 24–26. Furthermore, the adjusted phase-shift results, including saturation, and with appropriate values of $2k_F/k_p$, are in good qualitative agreement with $\rho(T)$ in the other low-resistivity amorphous alloys[22,23,25,26] which have been studied. On the other hand, although the Born-approximation results are within a factor of 2 of the observed magnitude of ρ, they fail to exhibit the temperature dependence of ρ observed in the low-resistivity amorphous alloys.

The following conclusions may be drawn from the above results.

(i) The diffraction model with appropriate matrix elements and incorporated phonon ineffectiveness effects at small $q\Lambda$ can explain the observed temperature dependence of ρ in low-resistivity ($\rho<100$ $\mu\Omega$ cm) amorphous alloys. Qualitative agreement with experiment is obtained if saturation effects are

neglected. This latter is to be contrasted with the situation in high-resistivity amorphous metals, where not even qualitative agreement with the observed temperature dependence of ρ can be obtained if saturation effects are not included in the diffraction model.

(ii) Saturation or Mooij effects are important even for resistivities as low as 50 $\mu\Omega$ cm. Moreover, the reduction in electron-phonon interaction (phonon ineffectiveness) can be adequately represented by the classically derived Pippard function[20] or even a sharp-cutoff form. Apparently a consistent procedure based upon a generalization of the diffraction model, which assumes that saturation effects in elastic scattering are negligible, describes the temperature dependence of the resisitivity equally well for alloys whose resistivity is 50 or 150 $\mu\Omega$ cm. This is particularly remarkable because it seems obvious that localization effects must eventually lead to a failure of this simple scattering picture and 150 $\mu\Omega$ cm corresponds to Λ of the order of interatomic spacings.

(iii) There is strong evidence that the Born approximation is not appropriate for studies of the temperature dependence of ρ in many disordered metals. Support for this is found in the studies of ρ in *a*-CuSn by Froböse and Jäckle,[10] the investigation of monovalent liquid metals by Young, Meyer, and Kilby,[36] the study of liquid Ca, Sr, and Ba by Ratti and Evans,[38] in addition to the present results.

ACKNOWLEDGMENTS

We thank Dr. U. Mizutani and Dr. T. Matsuda for their helpful comments and for providing data on *a*-MgZn prior to publication.

[1]J. M. Ziman, *Electrons and Phonons* (Clarendon, Oxford, 1960).

[2]T. E. Faber, *An Introduction to the Theory of Liquid Metals* (Cambridge University Press, London, 1972).

[3]G. Baym, Phys. Rev. 135, A1691 (1964).

[4]L. van Hove, Phys. Rev. 95, 294 (1954).

[5]T. E. Faber and J. M. Ziman, Philos. Mag. 11, 153 (1965).

[6]P. J. Cote and L. V. Meisel, in *Glassy Metals I,* edited by H.-J. Güntherodt and H. Beck (Springer, Heidelberg, 1981), pp. 141–166.

[7]P. J. Cote and L. V. Meisel, Phys. Rev. Lett. 39, 102 (1977).

[8]L. V. Meisel and P. J. Cote, Phys. Rev. B 16, 2978 (1977).

[9]L. V. Meisel and P. J. Cote, Phys. Rev. B 17, 4652 (1978).

[10]K. Froböse and J. Jäckle, J. Phys. F 7, 2331 (1977).

[11]S. R. Nagle, Phys. Rev. B 16, 1694 (1977).

[12]See, for example, *Electrons and Phonons,* Ref. 1, Chap. IX.

[13]J. H. Mooij, Phys. Status Solidi A 17, 521 (1973).

[14]Z. Fisk and G. W. Webb, Phys. Rev. Lett. 36, 1084 (1976).

[15]F. J. Ohkawa, J. Phys. Soc. Jpn. 44, 1105 (1978).

[16]N. Morton, B. W. James, and G. H. Westenholm, Cryogenics 18, 131 (1978).

[17]P. J. Cote and L. V. Meisel, Phys. Rev. Lett. 40, 1586 (1978).

[18]E.g., G. Bergmann and P. Marquardt, Phys. Rev. B 18, 326 (1978); Y. Waseda and H. S. Chen, Phys. Status Solidi B 87, 777 (1978); L. V. Meisel and P. J. Cote, Phys. Rev. B 15, 2970 (1977).

[19]E.g., P. B. Allen and B. Chakraborty, Phys. Rev. B 23, 4815 (1981).

[20]A. B. Pippard, Philos. Mag. 46, 1104 (1955). See also Chap. V of *Electrons and Phonons,* Ref. 1 and W. A. Fate, Ph.D thesis, Rensselaer Polytechnic Institute, 1967 (unpublished).

[21]E.g., M. Jonson and S. M. Girvin, Phys. Rev. Lett. 43, 1447 (1979); Y. Imry, Phys. Rev. Lett. 44, 469 (1980); W. L. McMillan, Phys. Rev. B 24, 2739 (1981).

[22]D. Korn, W. Murer, and G. Zibold, Phys. lett. 47A, 117 (1972).

[23]E. Blasberg, D. Korn, H. Pfeifle, J. Phys. F 9, 1821 (1979).

[24]T. Matsuda and U. Mizutani, in Proceedings of the Fourth International Conference on Rapidly Quenched Metals, Sendai, Japan, 1981 [J. Phys. F 12, 1877 (1982)]. Similar but less detailed resistivity results can be found in M. N. Baibich, W. B. Muir, Z. Altounian, and Tu Guo-Hua, Phys. Rev. B 26, 2963 (1982).

[25]T. Matsuda and U. Mizutani, Solid State Commun. 44, 145 (1982).

[26]U. Mizutani and T. Yoshida, J. Phys. F 12, 2331 (1982).

[27]J. Hafner, E. Gratz, and H.-J. Güntherodt, J. Phys. (Paris) Colloq. 41, C8-512 (1980).

[28]W. A. Harrison, *Pseudopotentials in the Theory of Metals* (Benjamin, New York, 1966), pp. 309ff. The pseudopotentials were calculated by A. E. O. Animalu based upon the method of V. Heine and I. V. Aberenkov, Philos. Mag. 9, 451 (1964).

[29]R. Evans, B. L. Gyorffy, N. Szabo, and J. M. Ziman, in *Properties of Liquid Metals,* edited by S. Takeushi (Wiley, New York, 1973). See also R. Evans, D. A. Greenwood, and P, Lloyd, Phys. Lett. A 35, 57 (1971).

[30]E.g., L. J. Sham and J. M. Ziman, in *Solid State Physics,* edited by F. Seitz and D. Turnbull (Academic, New York, 1963), Vol. 15; I. Hernandez-Calderone, J. S. Helman, and H. Vucetich, Phys. Rev. B 14, 2310 (1976).

[31]J. K. Percus and G. J. Yevick, Phys. Rev. 110, 1 (1957);

see also J. L. Lebowitz, Phys. Rev. 133, A1399 (1964).
[32]L. von Heimendahl, J. Phys. F 9, 161 (1979).
[33]J. M. Ziman, *Electrons and Phonons* (Clarendon, Oxford, 1960), p. 227.
[34]A. E. Dunsworth, Phys. Rev. B 12, 2030 (1975).
[35]See, for example, M. J. G. Lee and V. Heine, Phys. Rev. B 5, 2829 (1972), and the discussion in Ref. 34.
[36]W. H. Young, A. Meyer, and G. E. Kilby, Phys. Rev. 160, 160 (1967).
[37]See, for example, *An Introduction to the Theory of Liquid Metals,* Ref. 2, Table 5.2, or N. W. Ashcroft and J. Leckner, Phys. Rev. 145, 83 (1966).
[38]V. K. Ratti and R. Evans, J. Phys. F 13, L738 (1973).
[39]T. Mizoguchi, N. Shiotani, U. Mizutani, T. Kudo, and S. Yamada, J. Phys. (Paris) Colloq. 41, C8-183 (1980).
[40]U. Mizutani and T. Mizoguchi, J. Phys. F 11, 1385 (1981).